

## **WAVE-INDUCED GRAVEL AND COBBLE TRANSPORT ON A CRENULATE SHORELINE OF A LARGE INLET, GRAYS HARBOR, WASHINGTON**

Philip D. Osborne and Wei Chen

Pacific International Engineering, PLLC,  
123 Second Ave. South, P.O. Box 1599, Edmonds, WA, 98020, USA;  
e-mail: [philo@piengr.com](mailto:philo@piengr.com);  
phone: 425 921 1720  
fax: 425-744-1400;

### **KEYWORDS**

nearshore sediment transport, mixed sand-gravel-cobble beach, crenulate shoreline, CGWAVE, wave transformation model, magnetic particle tracer

### **ABSTRACT**

Gravel and cobble transport is investigated on a mixed sand, gravel and cobble beach at the head of a crenulate shaped shoreline by magnetic particle tracer measurements and a phase resolving wave model validated with local wave and current measurements. Net alongshore transport of gravel and cobble is generally several times greater than the net cross-shore transport at Half Moon Bay in Grays Harbor, Washington. Particle transport is a complex function of grain size because of rejection and overpassing of mid- to large-size particles and hiding of smaller particles (Osborne, in press). Wave transformation to the inner bank beach was simulated with the locally verified, phase resolving Coastal Gravity WAVE (CGWAVE) model to determine relevant wave parameters near the break point. Measured gravel and cobble transport is found to be directly correlated with variations in alongshore energy flux with most of the variance in transport being accounted for by the variance in the breaker wave height,  $H_b$ . The relationship between the cobble transport and  $H_b$  suggests the possibility of a threshold for alongshore transport at  $H_b$  equal to approximately 0.3 m. Because these conditions are equaled or exceeded a high percentage of the time on the inner bank shoreline, a larger cobble size would be required to provide a stable inner bank shoreline position.

### **1 INTRODUCTION**

Relatively few high quality field measurements of coarse-grained sediment transport are available from mixed-grain beaches with which to develop and validate predictive models (Bradbury and McCabe, 2003). Existing predictors for coarse- and mixed- grain sediment transport remain relatively crude and do not include a number of decisive factors such as swash and backwash hydrodynamics, infiltration, steep beach gradients, fractionation and differential hydraulic conductivity (e.g. Quick and Dyksterhuis, 1994; Van Wellen et al., 2000; Mason and Coates, 2001). Despite the lack of data and predictive ability, there is significant demand for design guidance on gravel and cobble and mixed beaches owing to their relative efficiency at dissipating wave energy and providing a natural or managed coastal defence (e.g. Bradbury and McCabe, 2003; Komar et al, 2003).

This paper presents an analysis of nearshore waves and coarse-grained sediment transport on a mixed sand, gravel and cobble transition beach at the head of a crenulate shaped bay, Half Moon Bay, of a large tidal inlet, Grays Harbor, Washington (Figure 1). Measurements of gravel and cobble transport were obtained during two particle tracer deployments in 2003 and 2004 (see Osborne, in press). The crenulate beach has been nourished with gravel and cobble as part of a breach repair thereby providing the opportunity to examine rates and patterns of sand, gravel and cobble transport in a relatively sheltered wave environment. The variations in wave height and wave angle that occur alongshore on a crenulate beach as a result of wave diffraction and refraction afford a wider range of experimental conditions within a relatively small spatial and temporal extent than could be achieved on an open coast beach. Prediction of wave transformations in this environment required application of the local-scale combined refraction-diffraction wave model: the Coastal Gravity WAVE (CGWAVE) model (e.g. Demirbilek and Panchang, 1998). The results provide data that are useful for the long term management of a nourished section and provide fundamental data for the development and testing of transport predictive formula.

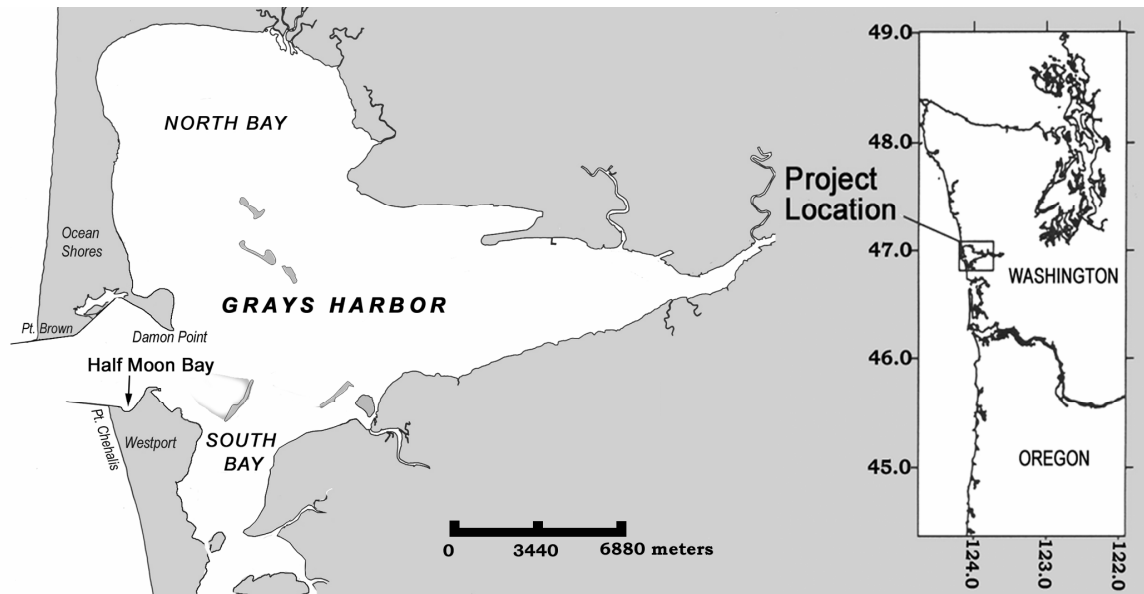


**Figure 1 Location of Grays Harbor and Half Moon Bay**

## 2 METHODS

The experimental layout for the field measurements is shown in Figure 2. Measurements included sampling of sediments for bed material characterization and tracer grain preparation, tracer grain experiments, beach profile surveying, and wave and current measurements. The size distribution of a surface sample (N=414) of gravel and cobble from the transition beach is shown as a histogram and cumulative frequency curve in Figure 3. Five particles from each of six size classes between large cobble (91 mm) and small pebble (16 mm), according to the Udden-Wentworth classification, were sampled at random from the overall surface sediment sample for each of the tracer particle sets. The details of bed material characterization, tracer grain preparation, and tracer deployments are described in Osborne (2005, in press) and in Osborne et al. (2003) and

are not re-iterated here; the main focus in this paper is the comparison of the particle tracer measurements with nearshore wave predictions. The particle tracer technique involved a combination of magnetic tracer particles and surveying with Real Time Kinematic Global Positioning System (RTK-GPS). The tracer experiments involved three sets of magnetic particle tracer deployments on 17 December 2003 and 9 February 2004.

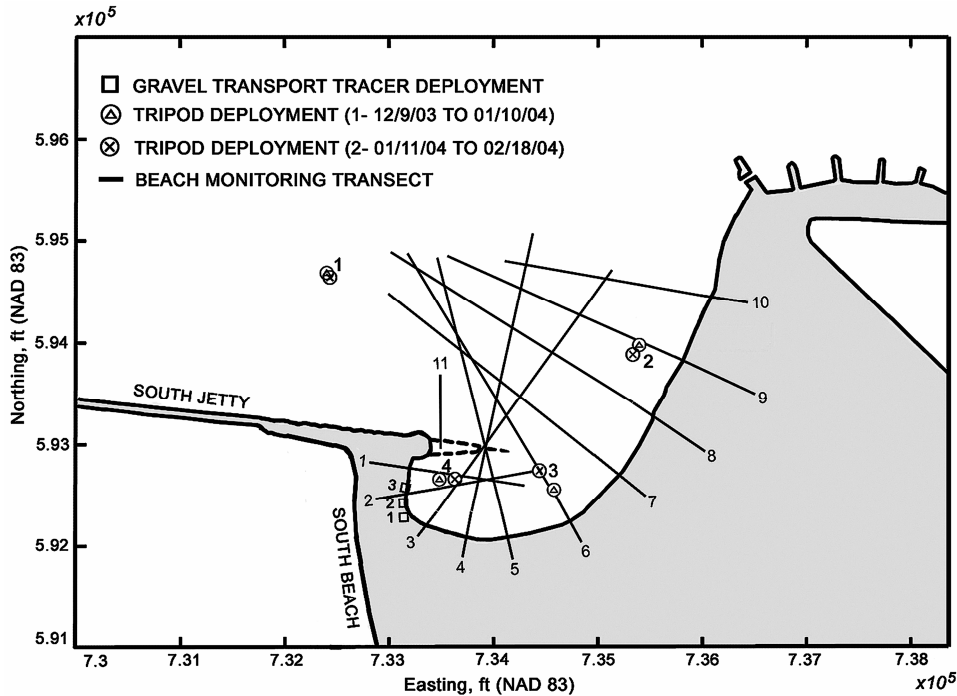
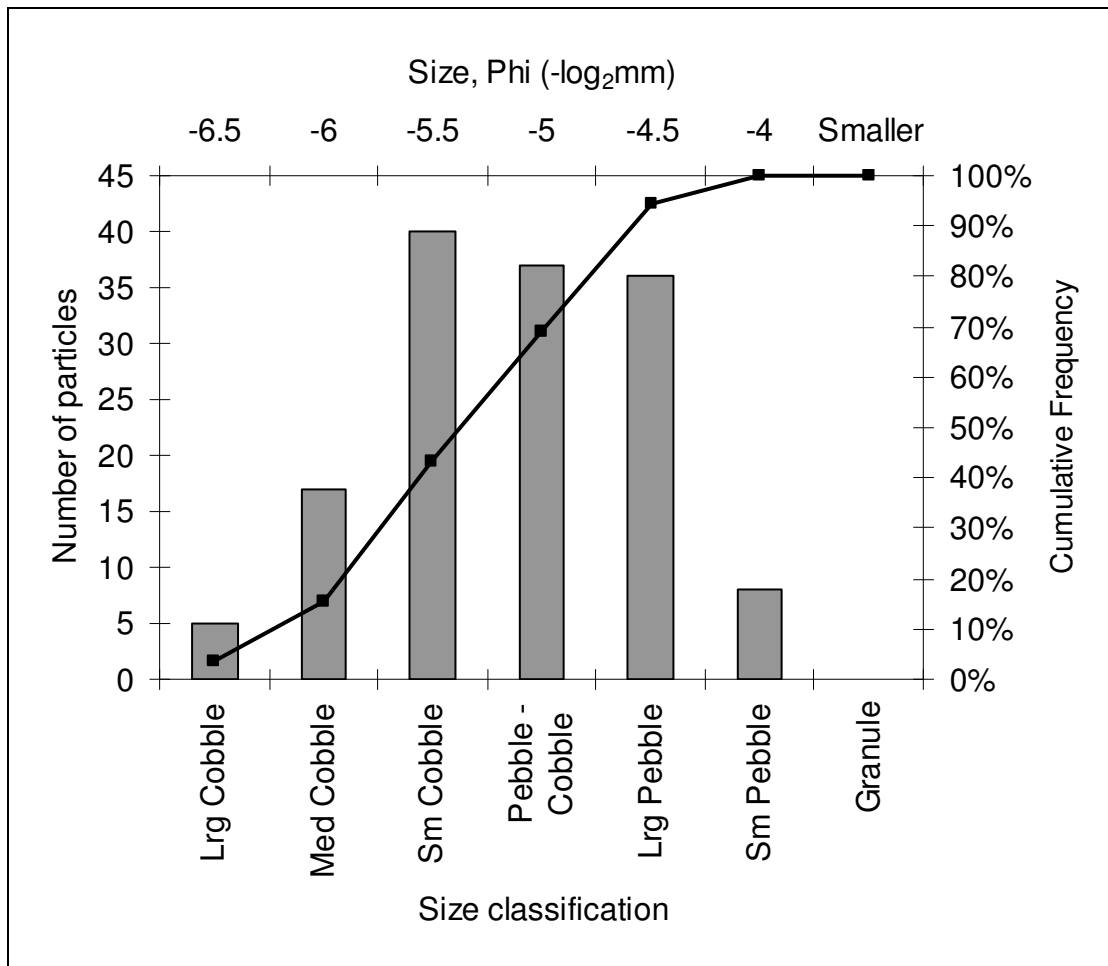


Figure 2 Experimental layout at Half Moon Bay



**Figure 3. Representative size distribution of a surface sample (N=414) of gravel and cobble from the transition beach.**

Measurements of directional waves, currents, and suspended sediment were obtained in Half Moon Bay concurrent with particle tracer measurements. Four instrument platforms were deployed (Figure 2) between 9 December 2003 and 19 February 2004 and equipped with an RD Instruments Sentinel Workhorse ADCP and Sontek Hydra systems. A directional wave buoy operated and maintained by the US Army Corps of Engineers and the Coastal Data Information Program (CDIP 036) located at 43 m depth approximately 1 km southwest of the entrance to Grays Harbor provided the directional wave boundary condition for a regional wave-current model (STWAVE-ADCIRC) that was used to transform waves to the inlet entrance. The latter model and its application to Grays Harbor is described in Cialone et al. (2002).

Time-series of significant wave height,  $H_s$ , peak period,  $T_p$ , and peak wave direction,  $D_p$ , measured at Half Moon Bay during the first set of tracer deployments are summarized in Figure 4. Waves during the deployments are characteristic of average winter conditions with average  $H_s$  of 3.4 m and  $T_p$  of 15.5 sec from the west and west-southwest. Systematic spatial variations in wave height and direction reflect the shoaling transformations, refraction and diffraction that occur as ocean waves enter Half Moon

Bay. Waves are turned from westerly to northwesterly as they enter the inlet (CDIP to Station (Stn) 1) and to northerly (Stn 1 to Stn 4) by refraction as they pass the terminus of south jetty. Waves are smallest at Stn 4 in the immediate lee of the jetty terminus and increase with distance along the crenulate bay shoreline progressing from Stn 4 to Stn 2.

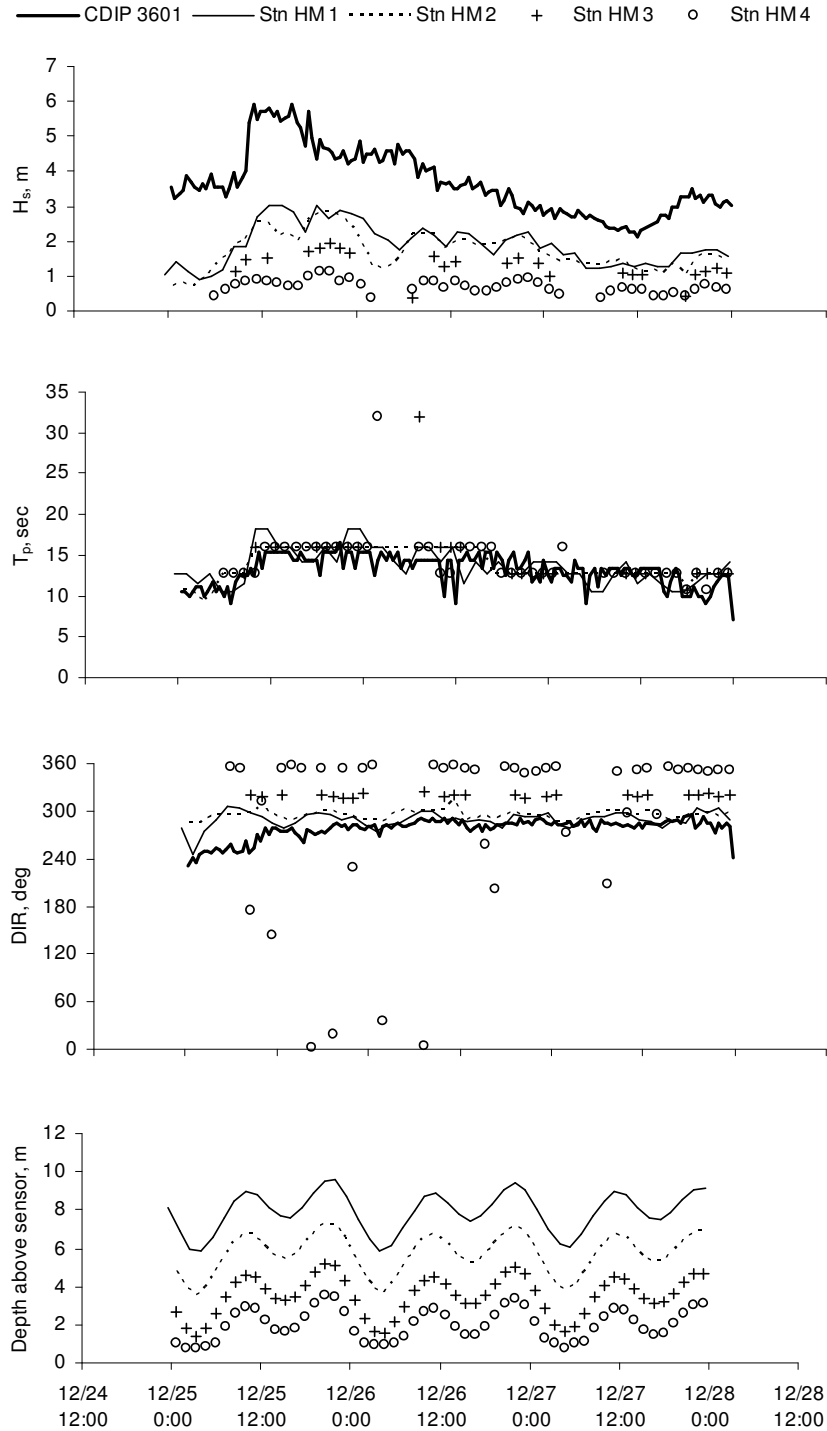


**Figure 4. Time series of  $H_s$ ,  $T_p$ , and  $D_p$ , and  $h$  measured at Half Moon Bay in December 2003.**

Few wave transformation models have the ability to simulate the relatively strong diffraction and refraction that occurs as waves propagate past the eastern terminus of the South Jetty; a more specialized wave model is required to simulate nearshore waves in Half Moon Bay at Grays Harbor. CGWAVE is a phase-resolving, finite element, coastal wave model based on the two-dimensional elliptic mild slope equation (Demirbilek and Panchang, 1998). CGWAVE simulates combined refraction-diffraction-reflection-dissipation (breaking and friction) caused by structures and bathymetry of arbitrary shape.

Figure 5 shows the CGWAVE model domain and bathymetry contours. The model domain was restricted to this region to avoid the need to include wave-current interaction in the model. Wave-current interactions in the inlet entrance are accounted for in the regional STWAVE-ADCIRC model. Particular attention was paid to developing the grid for the numerical model in the nearshore and inter-tidal zones of Half Moon Bay, and around the wave diffraction mound and jetty remnant area at the eastern terminus of South Jetty. Nearshore and inter-tidal bathymetry were supplemented with additional topographic survey information obtained from RTK-GPS surveys and shoreline positions interpreted from aerial photographs. A rectangular bathymetry grid with 25 ft horizontal grid spacing provided the basis for developing the computational grids.

Two FE meshes were developed: one for mean high water, mhw (mllw +2.48 m) and one for mean low water, mlw (mllw +0.13 m). Element resolution for each mesh was set to 12 nodes per wavelength based on a wave period of 12 sec and resulted in approximately 26,000 computational nodes. The largest element size for the domain was approximately 7.8 m and the smallest element size was approximately 1.35 m. The minimum depth in the model was set to 0.5 m.

Table 1 provides a comparison of the modeled wave heights with the measurements as well as with STWAVE predictions at the four measurement stations. Stn 1 provided validation of the incident waves for the regional STWAVE model, while Stn 2 to Stn 4 provided validation of CGWAVE. There is excellent agreement between CGWAVE model results and measurements for all three cases at all stations. The relative errors in wave height are within 10 percent for Case 1 and 2, and the wave direction is within 10 degrees. The wave height errors for Case 3 are somewhat larger (15 percent) but the wave angles agree within 10 degrees.

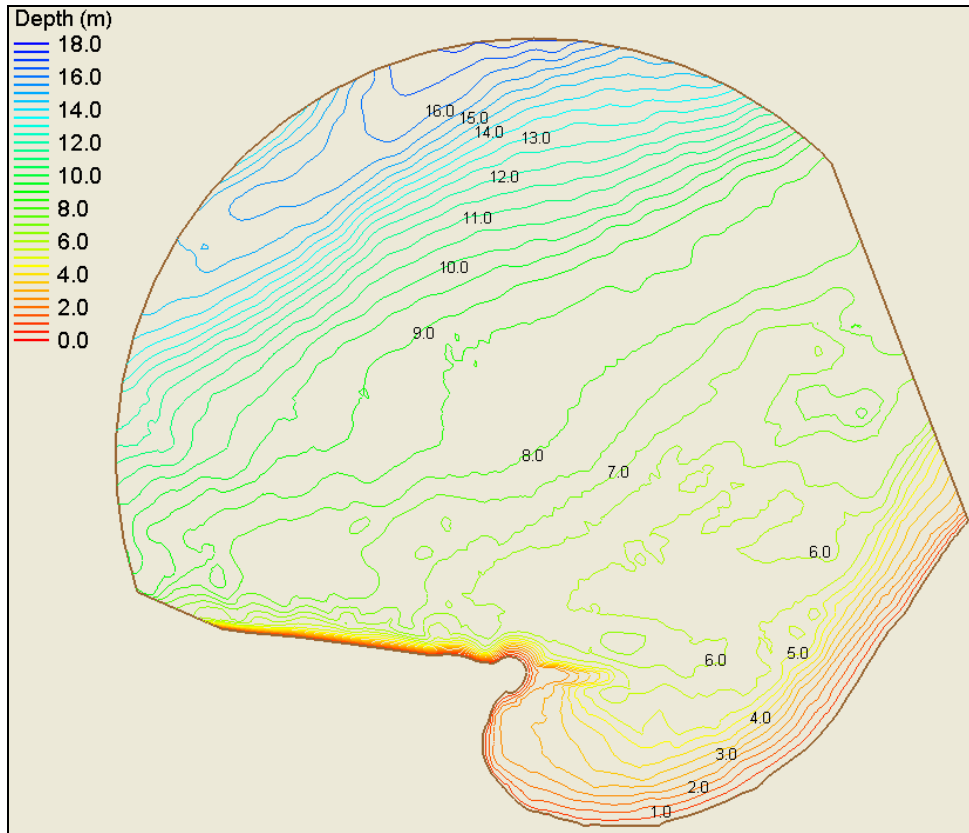


Figure 5. CGWAVE model domain and bathymetry contours

Table 1. Summary of CGWAVE verification

Case	Description		Stn 1		Stn 2		Stn 3		Stn 4	
			H, m	DIR						
1	high waves high tide	Measured	2.63	289	2.83	296	1.92	316	1.10	355
		CGWAVE	2.69	303	2.85	312	1.96	323	1.08	6
		STWAVE	3.04	334	2.91	322	1.08	303	0.44	296
2	Low waves high tide	Measured	1.37	288	1.27	299	1.02	320	0.62	353
		CGWAVE	1.38	298	1.31	309	0.92	320	0.54	358
		STWAVE	1.77	335	1.63	323	1.08	303	0.25	296
3	high waves low tide	Measured	3.05	286	2.18	289	N/A	N/A	0.71	358
		CGWAVE	3.00	295	1.89	305	N/A	N/A	0.33	36
		STWAVE	2.37	336	2.02	319	N/A	N/A	0.01	305

Wave height and wave angle relative to the shoreline at the breakpoint,  $H_b$  and  $\alpha_b$  respectively, are two parameters of relevance to beach morphodynamics and sediment transport. Longshore transport rate is also commonly estimated following the energy flux method (e.g. USACE, 1998). The longshore energy flux,  $P_l$ , a measure proportional to the longshore mass transport, is calculated as follows:

$$P_l = \frac{\rho g}{16} H_b^2 C_{gb} \sin 2\alpha_b$$

where  $C_{gb}$  is the local wave celerity and  $\alpha_b$  is calculated as the angle between local wave direction and the direction of the local seabed slope. Wave breaking in the CGWAVE model is calculated following Battjes (1973); the break-point in CGWAVE output is identified as the point at which a significant reduction of wave height occurs as the waves approach shore. The simple breaking criterion

$$H_b = 0.76h$$

where  $h$  is the water depth, was found to provide an adequate approximation of the position of the breaker line on the Half Moon Bay shoreline. Figure 6 shows an example of a breaker line position superimposed on the Half Moon Bay bathymetry; distances along the breaker line from the jetty terminus are also indicated.

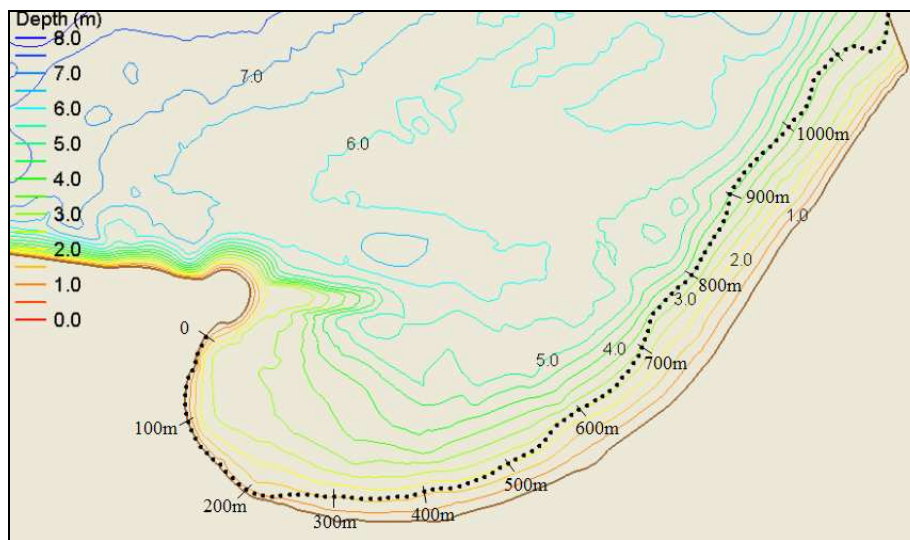


**Figure 6. Location of the breaker line at Half Moon Bay for the existing condition**

### 3 RESULTS

Figure 7 shows the particle transport paths for the deployment of particle tracer Set 1 that occurred during the two successive high tides between 17 December and 19 December 2003. The transport paths indicate a net transport alongshore to the south and east. The net alongshore transport is generally several times greater than the net cross-shore transport. The patterns for set 2 and 3 are similar to those for Set 1 (Osborne, in press). A relatively complex relationship between particle transport path length and particle size is evident in Figure 7. The particle transport patterns for various grain sizes implicate selective entrainment and the rejection (or overpassing) of mid- to large- sized particles in the distribution. Smaller particles are less exposed to fluid forces and prone to hiding or sheltering; the largest particles are simply more difficult to transport by fluid forces. The direct transport measurements are consistent with the overall particle size and shape distributions observed on this crenulate shaped inner bank beach whereby larger and

flatter particles have tended to outrun the smaller and more spherical particles in the downdrift direction (see Osborne, in press for more detail).

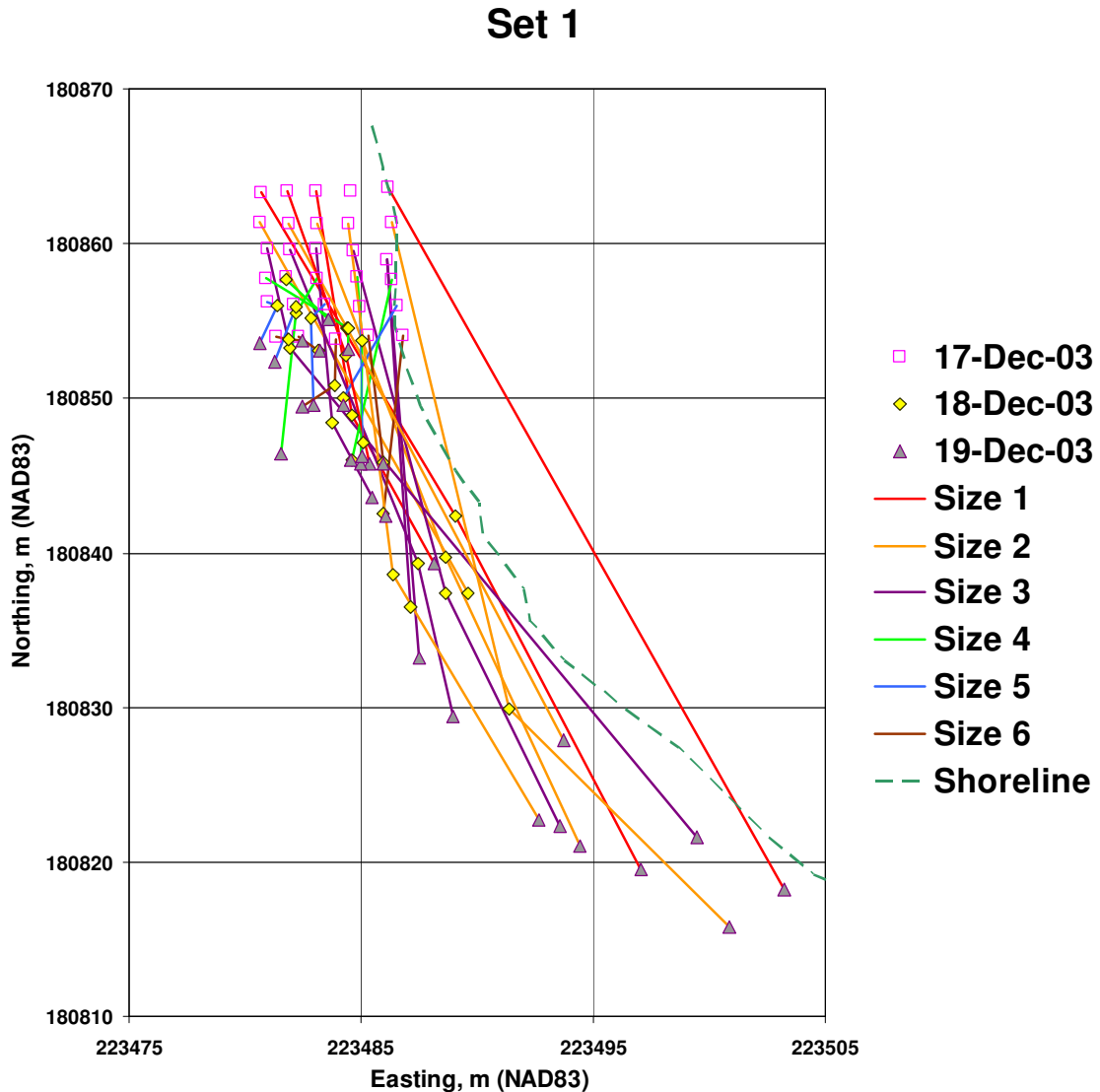


**Figure 7. Particle transport paths for difference size classes in Set 1 between 17 December 2003 and 19 December 2003**

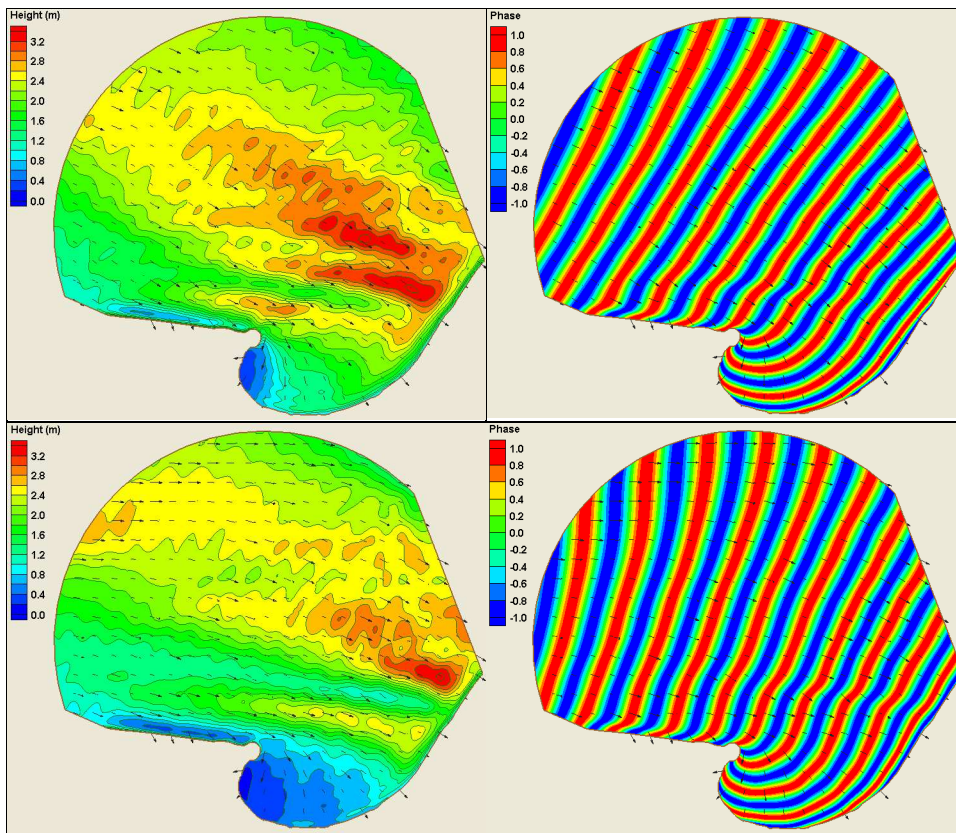
Predicted waves in the inlet entrance near measurement station Stn 1 (Figure 2) and the outer boundary of the CGWAVE grid (Figure 5) were extracted from STWAVE output for 6 cases corresponding to incident waves measured at CDIP 036. The cases are summarized in Table 2. The predicted waves were used to develop input conditions to the local CGWAVE model. Wave transformations were simulated with the local CGWAVE model to determine  $H_b$ ,  $T$ , and  $\alpha_b$  along breaker line at Half Moon Bay shoreline. Predictions of  $H_b$ ,  $T$ , and  $\alpha_b$  provided input for calculations of the longshore current velocity,  $V_L$ , and the longshore energy flux factor,  $P_L$ .

**Table 2. Summary of measured wave conditions for CGWAVE simulations**

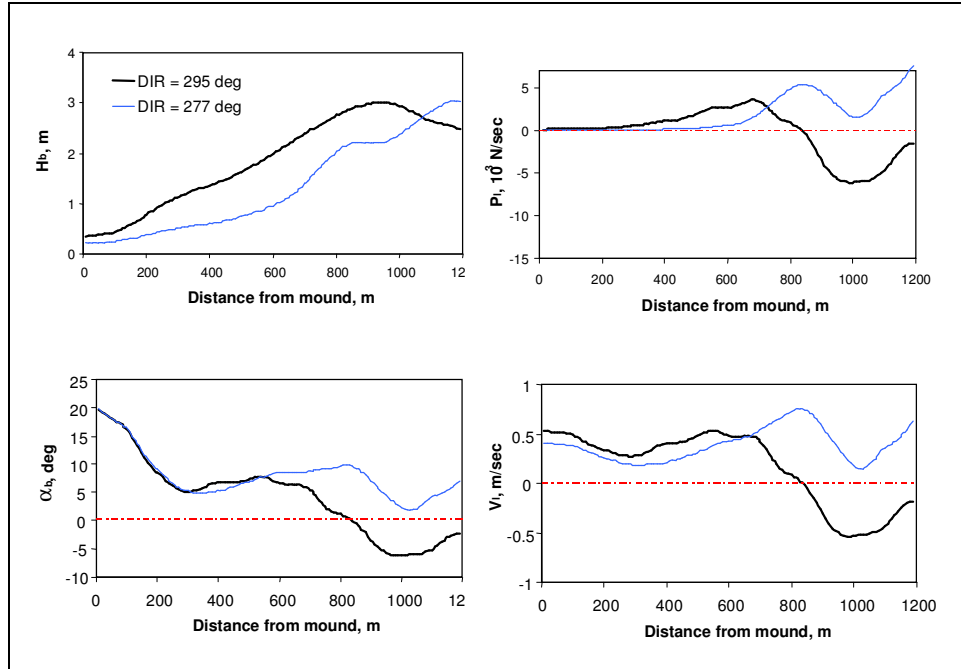
Case	From	To	CDIP			Stn 1			Stn 2			Stn 3			Stn 4		
			$H_s$ M	$T_p$ , sec	$D_p$ , deg-T												
1	12/17/2003	12/18/2003	2.7	15	275	1.2	14	292	1.1	15	298	0.6	14	318	0.5	15	276
2	12/18/2003	12/19/2003	2.6	14	259	0.9	15	226	0.9	14	294	0.6	16	319	0.4	14	209
3	2/9/2004	2/10/2004	2.5	14	275	N/A			1.1	13	292	0.8	13	312	0.5	12	335
4	2/10/2004	2/11/2004	2.1	14	273	N/A			1.1	14	292	0.8	13	314	0.6	13	335
5	2/11/2004	2/12/2004	1.5	13	273	N/A			0.8	14	293	0.5	14	312	0.4	14	337
6	2/12/2004	2/13/2004	1.6	11	261	N/A			0.6	12	290	0.4	13	310	0.4	13	335

Figure 8 shows maps of wave height, phase, and direction for Cases 1 and 5. The maps illustrate the effects of variation of wave angle at the outer boundary of the model domain between 277 deg and 295 deg. The analysis was performed to estimate of the sensitivity of numerical model results to incident wave angle. Figure 9 shows the variation in  $H_b$ ,  $\alpha_b$ ,  $V_b$ , and  $P_l$  with distance along the breaker line for the two cases shown in Figure 8.

The wave height maps and the plots of  $H_b$  along the breaker line indicate a region of reduced wave height in the southwest corner of the bay (in the lee of the diffraction mound at the jetty terminus). Progressively higher waves occur with distance away from the mound around the Half Moon Bay shoreline and reach a maximum in the nearshore area south of Stn 2 and the USCG Front Range tower (approximately 800 to 1000 m from the mound). The wave phase maps and variation in  $\alpha_b$  with distance along the breaker line indicate that waves approach the shoreline at a steep angle in the lee of the diffraction mound. Wave approach is generally more shore perpendicular along the Point Chehalis shoreline (600 m to 1000 m). The high wave angles in the southwest corner of Half Moon Bay have the potential to create a strong longshore current and large longshore flux potential. However, as indicated in Figure 9, the longshore flux potential is reduced in the immediate vicinity of the mound owing to the very small wave heights in that region. Flux potential and current speeds increase significantly with distance in the southwest corner of the bay as wave height increases.



**Figure 8. Maps of wave height and phase for offshore  $H_s = 4$  m,  $T = 16$  sec for Local  $DIR = 295$  deg (top) and Local  $DIR = 277$  deg (bottom)**



**Figure 9. Variation in  $H_b$ ,  $\alpha_b$ ,  $V_L$  and  $P_L$  with distance along the breaker line for offshore  $H_s = 4$  m,  $T = 16$  sec. (a) DIR = 277 deg; (b) DIR = 295 deg for the existing condition**

Gravel and cobble transport (expressed in terms of particle transport distance per tidal cycle) is directly correlated with variations in  $P_L$  with most of the variance being accounted for by the variance in  $H_b$ . Linear transport relationships (Figures 10 and 11) exhibit a direct dependence on the sediment size with mid- to large- sized sediments exhibiting greater transport distances for a given breaking wave height. The relationships between cobble transport and  $H_b$  for the various sediment sizes suggest a possible threshold for longshore transport of the cobble may exist at  $H_b$  of approximately 0.3 m.

#### 4 DISCUSSION AND CONCLUSIONS

Particle transport patterns at Half Moon Bay for various grain sizes implicate selective entrainment and the rejection (or overpassing) of mid- to large- sized particles in the distribution. Smaller particles are less exposed to fluid forces and prone to hiding or sheltering; the largest particles are simply more difficult to transport by fluid forces. These observations are consistent with beach observations that indicate a gradual long term depletion of the gravel and cobble nourishment in the southwest end of the bay and with alongshore patterns in particle shape and sorting (Osborne, in press).

Wave transformations to the inner bank beach may be simulated with a locally verified, phase resolving model that incorporates refraction and diffraction processes such as the Coastal Gravity WAVE (CGWAVE) model. In this paper the model is applied to determine relevant wave parameters near the break point. Measured gravel and cobble transport is found to be directly correlated with variations in alongshore energy flux with most of the variance in transport being accounted for by the variance in the breaker wave

height,  $H_b$ . The relationship between the cobble transport and  $H_b$  suggests the possibility of a threshold for alongshore transport at  $H_b$  equal to approximately 0.3 m. Because these conditions are equaled or exceeded a high percentage of the time on the inner bank shoreline, a larger cobble size would be required to provide a stable inner bank shoreline position.

These conditions are equaled or exceeded a high percentage of the time in the southwest corner of Half Moon Bay. The results indicate that a larger cobble size would be required to provide a statically stable cobble berm in the transition region.

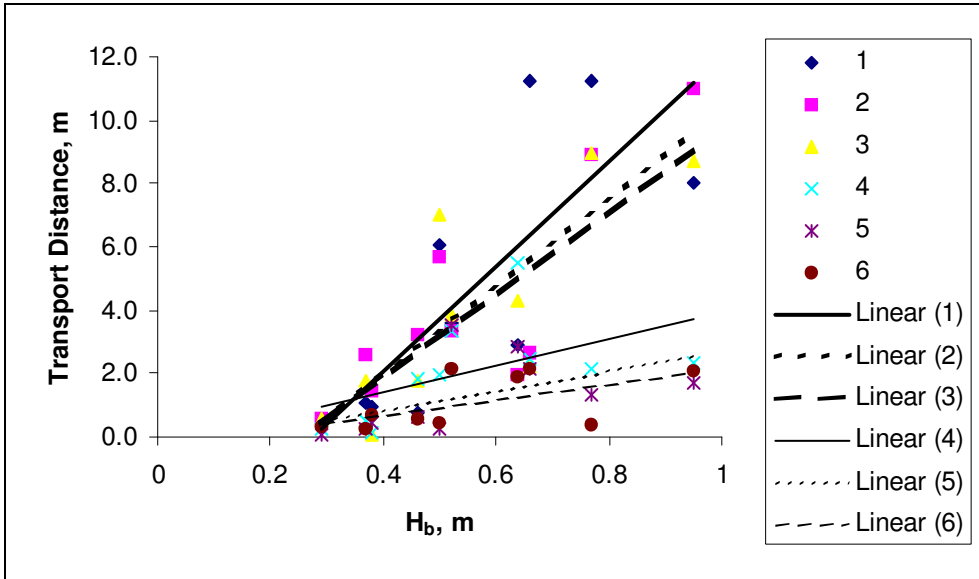


Figure 10. Transport distance of gravel and cobble per tidal cycle as a function of  $H_b$  for the range of size classes (1 through 6) defined in Table 1.

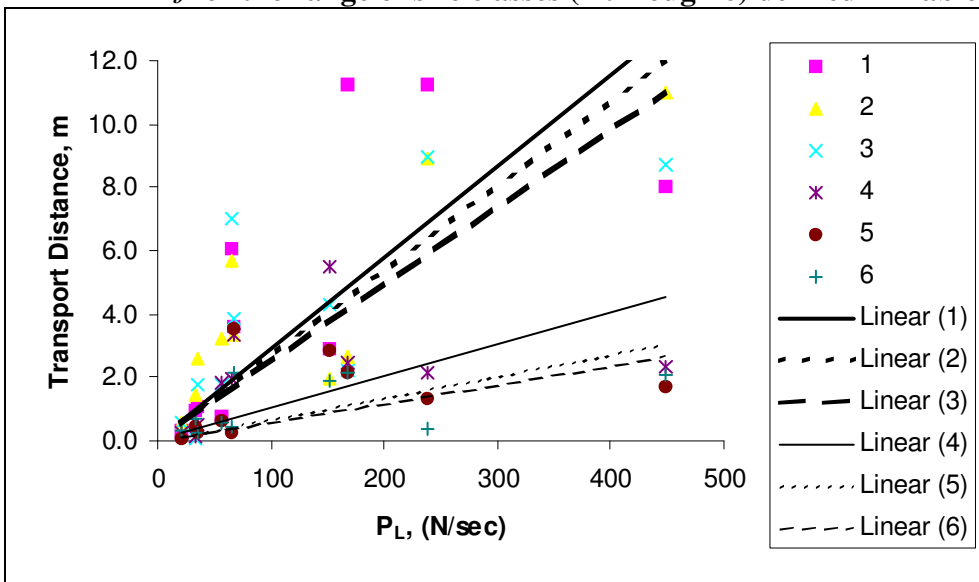


Figure 11. Transport distance of gravel and cobble per tidal cycle as a function of  $P_L$  for the range of size classes (1 through 6) defined in Table 1.

**ACKNOWLEDGEMENTS**

Funding for the field experiments and modeling was provided by ERDC-CHL under contract DACW 42-03-C-0028 and a grant from the Coastal Inlets Research Program. The authors are grateful to David Hericks and Robert Osborne of Pacific International Engineering, PLLC, for assistance with the field measurements and to Dr Nicholas Kraus of ERDC-CHL for useful discussion of the paper.

**REFERENCES**

- Battjes, J.A. (1973). Set-up due to irregular waves. Proc. 13<sup>th</sup> Int. Conf. Coastal Eng., ASCE., pp. 1993-2004.
- Bradbury, A.P. and McCabe, M. (2003). Morphodynamic Response of Shingle and Mixed Sand/Shingle Beaches in Large Scale Tests – Preliminary Observations, Conference Paper – Hydrolab II, Budapest, 22-23 May 2003, pp. 9-1 to 9-11.
- Cialone, M.A., Millitello, A., Brown, M.E., and Kraus, N.C. 2002. Coupling of wave and circulation numerical models at Grays Harbor entrance, Washington, USA.. *Proc. 28<sup>th</sup> ICCE 2002*, World Scientific, 1279-1291.
- Demirbilek, Z., Xu, B., and Panchang, V. (1998). “CGWAVE: A coastal surface water wave model of the mild-slope equation,” Technical Report CHL-98-26, Coastal and Hydraulics Laboratory, US Army Engineer Research and Development Center, Vicksburg, MS.
- Komar, P.D., Allan, J.C. and Winz, R. (2003). Cobble Beaches – The Design with Nature Approach for Shore Protection, Proceedings of Coastal Sediments '03, Clearwater Beach, FL, available on CDROM.
- Mason, T. and Coates, T.T. (2001). Sediment Transport Processes on Mixed Beaches: A Review for Shoreline Management, *Journal of Coastal Research*, 17(3), pp. 645-657.
- Osborne, P.D. (in press). Transport of gravel and cobble on a mixed-sediment inner bank shoreline of a large inlet, Grays Harbor, Washington. *Marine Geology: Revised manuscript accepted for publication, August, 2005.*
- Osborne, P.D., Wamsley, T.V. and Arden, H.T. (2003). “South Jetty Sediment Processes Study, Grays Harbor Washington: Evaluation of Engineering Structures and Maintenance Measures”, US Army Corps of Engineers, Engineering Research and Development Center, Coastal and Hydraulics Laboratory, ERDC/CHL TR-03-4.
- Quick, M.C. and Dyksterhuis, P. (1994). Cross-shore Transport for Beaches of Mixed Sand and Gravel, *International Symposium: Waves-Physical and Numerical Modeling (Canadian Society of Civil Engineers)*, pp. 1443-1452.
- USACE, 1998. Coastal Engineering Manual, Part III, Chapter 2, Longshore Sediment Transport. EC 1110-2-292, US Army Corps of Engineers, Washington, DC.

Van Wellen, E.V., Chadwich, A.J. and Mason, T. (2000). "A Review and Assessment of Longshore Sediment Transport Equations for Coarse-Grained Beaches", *Coastal Engineering* (40), pp. 243-275.